Potential Surfaces for Unimolecular and Bimolecular Gas Phase Reactions of BH_mCl_n Calculated at the G2 Level of Theory

H. Bernhard Schlegel* and Anwar G. Baboul

Department of Chemistry, Wayne State University, Detroit, Michigan 48202

Stephen J. Harris

Physical Chemistry, General Motors Research & Development, Warren, Michigan 48090-9055

Received: February 5, 1996; In Final Form: March 5, 1996[⊗]

Transition structures and reaction paths for the BH_mCl_n system have been characterized at the MP2(full)/6-31G(d) level of theory; heats of reaction and barriers have been computed at the G2 level of theory. Calculations show that the insertion reactions of BH_mCl_n into H_2 and HCl ($m + n = 0, 1, 2$) occur by highly distorted, non-least motion transition states, with barriers that increase with chlorine substitution on boron. Hydrogen abstraction from BH and $BH_{3-n}Cl_n$ by chlorine proceeds with little or no barrier by a linear transition state. By contrast, $BH_{3-n}Cl_n + H \rightarrow BH_{2-n}Cl_n + H_2$ occurs by an addition−elimination path via a tetracoordinate intermediate. Likewise, $BH_{2-n}Cl_n + X \rightarrow BH_{1-n}Cl_n + HX$ or $BH_{2-n}Cl_{n-1} + XCl$ (X = H, Cl) are also addition−elimination processes. Abstraction of Cl from BCl and $BH_{3-n}Cl_n$ by H is endothermic and occurs by a bent transition state.

Introduction

Boron compounds such as cubic boron nitride, boron carbide, and titanium diboride are among the hardest and most abrasion-resistant materials. Like diamond, these materials also have low densities, high melting points, and considerable mechanical strength and are chemically inert. As a result, they can make excellent wear- and corrosion-resistant coatings.[1] Boron-containing films can be grown using chemical vapor deposition (CVD). Because of the extreme toxicity associated with boron hydrides, BCl_3 has been a commonly used boron precursor in CVD. Although there have been a number of publications examining the chemistry and kinetics of CVD film formation from BCl_3, the validity of these analyses is uncertain because of a lack of accurate, relevant experimental or theoretical data on the decomposition of BCl_3. For example, one of the most careful and detailed studies of boron carbide formation with CVD techniques modeled the chemistry and the fluid mechanics in a $BCl_3/CH_4/H_2$ stagnation flow system with just two gas phase and two gas−surface reactions[2]

$$BCl_3 + H_2 \rightarrow BHCl_2 + HCl$$

$$BHCl_2 \rightarrow BCl + HCl$$

$$BCl + {}^1/_2H_2 \rightarrow B_s + HCl$$

$$CH_4 \rightarrow C_s + 2H_2 \qquad (1)$$

However, because of a lack of experimental or theoretical data for these species, there is in fact no evidence that any of these global reactions play a role in the formation of boron carbide. CVD reaction schemes leading to formation of boron nitride from BCl_3 are of necessity similarly crude.

We have recently used quantum calculations at the G2 level of theory to provide a self-consistent set of heats of formation and vibrational frequencies for BH_mCl_n ($0 \le m, n \le 3$).[3] These data can form part of the foundation for accurate modeling of BCl_3 decomposition chemistry in the presence of H_2, but kinetic information is also required. Figure 1 summarizes the unimolecular and bimolecular reactions that could interconvert the different species in the BH_mCl_n system. Experimental rate data are available for $BH + H_2$[4,5] and $BCl_3 + H$[6] but not for most of the other reactions in Figure 1. The $BH + H_2 \rightarrow BH_3$ reaction has also been studied by high-level electronic structure methods.[5] The reaction path and potential energy surface were obtained by CASSCF and MRCI calculations with large, correlation consistent basis sets. The theoretical rate constant and activation energy are in excellent agreement with experiment. The rates for $BCl + H$, $BCl + Cl$, $BH + H$, $BH + Cl$, and $B + Cl_2$ have also been examined but only using empirical BEBO surfaces.[7,8] There are no systematic, high-level studies that treat the reactions of BH_mCl_n in a uniform and consistent manner. Theoretical methods such as the G2 level of theory are capable of calculating energetics of small gas phase species to within 1−2 kcal/mol.[9−11] Previously, we have used this level of theory to calculate the heats of formation of BH_mCl_n.[3] In this paper, we use the same approach to investigate the transition structures and reaction barriers in the BH_mCl_n system.

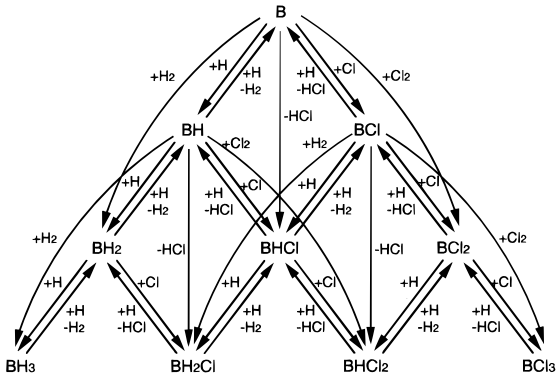

Figure 1. Potential reactions interconverting species in the BH_mCl_n system.

[⊗] Abstract published in *Advance ACS Abstracts,* May 1, 1996.

S0022-3654(96)00347-4 CCC: $12.00

TABLE 1: Total Energies (hartrees) for Reactants, Intermediates, and Transition States in the BH_mCl_n System[a]

species	sym	MP2(full)/6-31G(d)[b]	G2[c]
reactants and intermediates			
BH	$C_{\infty v}$	−25.175 870	−25.233 699
BCl	$C_{\infty v}$	−484.311 686	−484.474 419
BH_2	C_{2v}	−25.808 445	−25.856 344
BHCl	C_s	−484.911 069	−485.067 923
BCl_2	C_{2v}	−944.008 108	−944.274 167
BH_3	D_{3h}	−26.468 568	−26.523 328
BH_2Cl	C_{2v}	−485.570 245	−485.733 340
$BHCl_2$	C_{2v}	−944.668 094	−944.940 296
BCl_3	D_{3h}	−1403.759 581	−1404.141 597
BH_2-H_2	C_{2v}	−26.977 691	−27.046 430
$BHCl-H_2$	C_s	−486.069 302	−486.244 956
BCl_2-H_2	C_{2v}	−945.162 373	−945.445 738
insertions transition states			
$B + H_2 \rightarrow BH_2$	C_s	−25.658 867	−25.737 081
$BH + H_2 \rightarrow BH_3$	C_s	−26.309 448	−26.392 132
$BCl + H_2 \rightarrow BH_2Cl$	C_s	−485.396 447	−485.589 758
$BH_2 + H_2 \rightarrow BH_2-H_2$	C_s	−26.951 144	−27.021 788
$BHCl + H_2 \rightarrow BHCl-H_2$	C_1	−486.041 908	−486.223 151
$BCl_2 + H_2 \rightarrow BCl_2-H_2$	C_s	−945.128 278	−945.421 062
$B + HCl \rightarrow BHCl$	C_s	−484.752 255	−484.942 865
$BH + HCl \rightarrow BH_2Cl$	C_s	−485.384 834	−485.576 476
$BCl + HCl \rightarrow BHCl_2$	C_s	−944.505 180	−944.804 380
hydrogen abstractions transition states			
$BH + H \rightarrow B + H_2$	$C_{\infty v}$	−25.656 946	−25.726 773
$BH_3 + H \rightarrow BH_2 + H_2$[d]	C_{2v}	−26.929 235	−27.003 450
$BH_2Cl + H \rightarrow BHCl + H_2$	C_s	−486.032 256	−486.214 703
$BHCl_2 + H \rightarrow BCl_2 + H_2$	C_{2v}	−945.130 842	−945.421 631
$BH_3 + Cl \rightarrow BH_2 + HCl$	C_{2v}	−486.010 676	−486.199 347
$BH_2Cl + Cl \rightarrow BHCl + HCl$	C_s	−945.133 354	−945.411 155
$BHCl_2 + Cl \rightarrow BCl_2 + HCl$	C_{2v}	−1404.210 355	−1404.616 958
chlorine abstractions transition states			
$BCl + H \rightarrow B + HCl$	C_s	−484.740 574	−484.933 030
$BH_2Cl + H \rightarrow BH_2 + HCl$	C_s	−486.009 238	−486.200 321
$BHCl_2 + H \rightarrow BHCl + HCl$	C_1	−945.100 220	−945.400 346
$BCl_3 + H \rightarrow BCl_2 + HCl$	C_s	−1404.188 613	−1404.598 971

[a] Additional MP2[b] and G2[c] energies: H −0.498 230, −0.500 000; B −24.562 460, −24.602 05; Cl −459.562 060, −459.676 640; H_2 −1.144 141, −1.165 863; HCl −460.202 149, −460.339 955. [b] Without ZPE. [c] At 0 K, with ZPE using MP2(full)/6-31G(d) frequencies scaled by 0.9646 rather than HF/6-31G(d) frequences. [d] Second-order saddle point.

Method

Molecular orbital calculations were carried out using the GAUSSIAN 94[12] series of programs using a variety of basis sets of split valence quality or better with multiple polarization and diffuse functions[13] and spin-unrestricted methods. Equilibrium geometries were optimized by Hartree−Fock and second-order Møller−Plesset perturbation theory (HF/6-31G(d) and MP2(full)/6-31G(d), respectively) using a quasi-Newton optimization method.[14] Vibrational frequencies and zero-point energies were calculated at the HF/6-31G(d) and MP2(full)/6-31G(d) levels using analytical second derivatives.[15,16] All transition states had only one imaginary frequency. Some representative transition states were characterized further by reaction path following[17] to confirm the nature of the reactants and products of the reaction. Correlated energies were calculated by fourth-order Møller−Plesset perturbation theory[18] (MP4SDTQ, frozen core) and by quadratic configuration interaction with perturbative correction for triple excitations[19] (QCISD(T), frozen core) with the MP2(full)/6-31G(d) optimized geometries. In the G2 method,[9,10] the energy computed at MP4/6-311G(d,p) is corrected for the effect of diffuse functions obtained at MP4/6-311+G(d,p) and MP2/6-311+G(3df,2p), for the effect of higher polarization functions obtained at MP4/6-311G(2df,p) and MP2/6-311+G(3df,2p), and for the effect of electron correlation beyond fourth-order obtained at QCISD(T)/6-311G(d,p). Higher level corrections for deficiencies in the wave function are estimated empirically[9,10] based on the number of paired and unpaired electrons.

$$E(\mathrm{G2}) = E(\mathrm{MP4/6\text{-}311G(d,p)}) + \Delta E(\mathrm{diffuse}) + \Delta E(\mathrm{polarization}) + \Delta E(\mathrm{QCI}) + \Delta E(\mathrm{HLC}) + \mathrm{ZPE} \quad (2)$$

The average absolute error of the additivity assumptions in the G2 level of theory is only 0.30 kcal/mol.[11] Because the geometry and frequencies of some transition states are sensitive to the level of theory, in the present work we use the zero-point energy calculated at the MP2/6-31G(d) scaled by 0.9646[20] for all structures (minima and transition states) rather than the HF/6-31G(d) zero-point energy scaled by 0.8929.[21] At the G2 level of theory, the mean absolute error for 125 well-characterized atomization energies, ionization energies, electron affinities, and proton affinities is 1.3 kcal/mol.[10] The errors for barrier heights are probably similar or somewhat larger.

Results and Discussion

The reactions in Figure 1 can be grouped into three basic categories: homolytic bond cleavage reactions, radical abstractions, and insertion (or 1,1-elimination) reactions. Some of the reactions in Figure 1 can also occur by an addition−elimination process. The reverse of the bond cleavage, radical addition reactions, should have little or no barrier. Hence, we did not search for a classical transition state on the potential energy surface for these reactions (however, a variational transition state would exist on the free energy surface).

The MP2 and G2 energies of various stationary points on the BH_mCl_n surface are listed in Table 1. Most of the open-shell species have S^2 values of 0.75−0.85, except the transition states for B + H_2, B + HCl, and BCl + H, which are in the range 0.95−1.1. The geometries optimized at the MP2(full)/6-31G(d) level are given in Figures 2−8. While this level of theory is usually quite satisfactory for equilibrium geometries, the geometries of some transition states may improve with larger basis sets and higher levels of theory. The harmonic vibrational

TABLE 2: Moments of Inertia and Frequencies for Reactions, Intermediates, and Transition States[a]

reactants and intermediates	
BH	5.017
	2448.4
BCl	87.854
	880.2
BH_2	1.675, 8.183, 9.858
	1080.2, 2688.3, 2847.9
BHCl	3.017, 101.764, 104.781
	884.3, 969.9, 2744.9
BCl_2	21.187, 583.362, 604.549
	299.7, 742.1, 1034.5
BH_3	7.667, 7.667, 15.333
	1191.8, 1255.1, 1255.1, 2646.9, 2789.8, 2789.8
BH_2Cl	7.872, 114.279, 122.151
	868.5, 919.7, 1044.2, 1291.2, 2709.7, 2826.4
$BHCl_2$	37.659, 568.834, 606.493
	308.6, 772.8, 824.3, 953.7, 1167.2, 2792.8
BCl_3	564.086, 564.086, 1128.172
	272.6, 272.6, 479.9, 496.9, 1009.1, 1009.1
BH_2-H_2	10.342, 13.238, 19.206
	803.1, 858.1, 889.5, 1109.0, 1321.7, 2110.5, 2224.2, 2731.9, 2852.9
$BHCl-H_2$	13.251, 130.938, 137.676
	685.0, 777.2, 810.2, 855.3, 939.4, 1221.0, 1963.8, 2201.9, 2784.6
BCl_2-H_2	50.878, 588.745, 631.568
	289.5, 491.8, 740.5, 821.0, 829.5, 955.4, 1015.3, 1914.8, 2211.4
insertions transition states	
$B + H_2 \rightarrow BH_2$	2.527, 13.286, 15.813
	1100.4*i*, 698.3, 2195.7
$BH + H_2 \rightarrow BH_3$	6.038, 15.536, 21.574
	626.4*i*, 911.9, 1104.4, 1423.3, 2517.9, 3293.4
$BCl + H_2 \rightarrow BH_2Cl$	9.391, 114.631, 124.022
	1446.5*i*, 669.1, 871.3, 935.0, 1450.0, 2509.1
$BH_2 + H_2 \rightarrow BH_2-H_2$	10.748, 26.237, 31.970
	388.5*i*, 310.7, 616.4, 688.2, 917.5, 1039.5, 2703.0, 2866.1, 4291.5
$BHCl + H_2 \rightarrow BHCl-H_2$	19.134, 132.513, 145.092
	695.5*i*, 503.3, 589.5, 763.4, 845.2, 964.7, 1112.6, 2783.4, 3904.8
$BCl_2 + H_2 \rightarrow BCl_2-H_2$	53.919, 599.387, 641.209
	805.0*i*, 283.2, 459.1, 575.2, 702.7, 806.1, 1001.4, 1225.5, 3331.1
$B + HCl \rightarrow BHCl$	2.304, 184.119, 186.422
	879.9*i*, 333.1, 1470.2
$BH + HCl \rightarrow BH_2Cl$	4.972, 269.385, 274.357
	487.5*i*, 225.6, 766.1, 780.4, 1432.5, 2624.7
$BCl + HCl \rightarrow BHCl_2$	41.635, 898.382, 940.018
	737.2*i*, 118.5, 518.8, 735.5, 962.6, 1572.1
hydrogen abstractions transition states	
$BH + H \rightarrow B + H_2$	25.515, 25.515
	2015.4*i*, 1020.5, 1020.5, 1160.6
$BH_3 + H \rightarrow BH_2 + H_2$[b]	8.023, 30.092, 38.116
	1749.3*i*, 386.7*i*, 389.7, 1122.0, 1180.3, 1207.5, 1602.9, 2688.4, 2832.1
$BH_2Cl + H \rightarrow BHCl + H_2$	23.267, 137.120, 160.387
	1764.9*i*, 88.2, 236.3, 883.5, 956.8, 1184.9, 1223.4, 1598.2, 2750.4
$BHCl_2 + H \rightarrow BCl_2 + H_2$	73.465, 578.697, 652.163
	1728.1*i*, 133.0, 220.3, 298.5, 707.6, 1008.8, 1158.9, 1219.4, 1629.9
$BH_3 + Cl \rightarrow BH_2 + HCl$	8.398, 331.911, 340.308
	568.8*i*, 229.3, 248.0, 817.6, 925.9, 958.8, 1093.4, 2718.6, 2895.5
$BH_2Cl + Cl \rightarrow BHCl + HCl$	57.702, 1073.396, 1131.098
	514.5*i*, 83.5, 240.0, 769.5, 815.3, 900.6, 940.2, 1056.7, 2779.8
$BHCl_2 + Cl \rightarrow BCl_2 + HCl$	588.839, 1190.769, 1779.608
	435.9*i*, 62.2, 151.1, 260.6, 640.6, 716.8, 828.9, 1043.9, 1096.2
chlorine abstractions transition states	
$BCl + H \rightarrow B + HCl$	4.354, 115.024, 119.378
	1070.4*i*, 647.5, 1063.3
$BH_2Cl + H \rightarrow BH_2 + HCl$	13.590, 136.187, 139.155
	940.1*i*, 452.8, 623.0, 766.6, 869.1, 1070.1, 1337.9, 2713.3, 2861.8
$BHCl_2 + H \rightarrow BHCl + HCl$	51.607, 608.976, 649.492
	846.8*i*, 238.7, 395.6, 542.5, 751.4, 871.2, 1037.9, 1455.3, 2790.0
$BCl_3 + H \rightarrow BCl_2 + HCl$	591.793, 627.800, 1201.123
	830.6*i*, 195.1, 209.6, 308.3, 388.2, 539.5, 766.8, 977.4, 1337.9

[a] For each entry: first line, moments of inertia (amu $bohr^2$); second line, frequencies (cm^{-1}); based on ^1H, ^{11}B, and ^{35}Cl; additional values: H_2, 0.979, 4532.4; HCl, 5.733, 3046.5. [b] Second-order saddle point.

frequencies and moments of inertia calculated at the MP2(full)/6-31G(d) level are listed in Table 2. The calculated vibrational frequencies at this level of theory are typically ca. 6% too high[20] when compared to observed frequencies because of basis set effects, the neglect of electron correlation, and vibrational anharmonicity. Heats of reaction and barrier heights are given in Table 3. For some reactions, there may be weakly bound reactant-like clusters, allowing the transition states to be slightly lower than separated reactants. Note that recent experiments[22,23] and calculations[4,24] indicate that the heat of formation of gas

TABLE 3: Heats of Reaction and Barrier Heights in the BH_mCl_n System[a]

	heats of reaction		forward barrier		reverse barrier	
species	MP2	G2	MP2	G2	MP2	G2
insertions transition states						
$B + H_2 \rightarrow BH_2$	−63.9	−55.5	30.0	19.3	93.9	78.8
$BH + H_2 \rightarrow BH_3$	−93.2	−77.7	6.6	4.6[b]	99.8	82.3
$BCl + H_2 \rightarrow BH_2Cl$	−71.8	−58.4	37.3	31.7	109.1	90.1
$BH_2 + H_2 \rightarrow BH_2-H_2$	−15.8	−15.2	0.9	0.4	16.6	15.6
$BHCl + H_2 \rightarrow BHCl-H_2$	−8.8	−7.0	8.4	6.7	17.2	13.7
$BCl_2 + H_2 \rightarrow BCl_2-H_2$	−6.4	−3.6	15.0	12.0	21.4	15.6
$B + HCl \rightarrow BHCl$	−91.9	−79.0	7.8	−0.5	99.7	78.5
$BH + HCl \rightarrow BH_2Cl$	−120.6	−100.2	−2.2	−1.8	118.5	98.4
$BCl + HCl \rightarrow BHCl_2$	96.8	−79.0	5.4	6.3	102.2	85.3
hydrogen abstractions transition states						
$BH + H \rightarrow B + H_2$	−20.4	−21.5	10.8	4.3	31.2	25.8
$BH_3 + H \rightarrow BH_2 + H_2$[c]	8.9	0.7	23.6	12.5	14.7	11.8
$BH_2Cl + H \rightarrow BHCl + H_2$	8.3	−0.3	22.7	11.7	14.4	12.0
$BHCl_2 + H \rightarrow BCl_2 + H_2$	8.8	0.2	22.3	11.7	13.4	11.5
$BH + Cl \rightarrow B + HCl$	12.6	2.3	12.5	0.4	−0.1	1.9
$BH_3 + Cl \rightarrow BH_2 + HCl$	12.6	2.3	12.5	0.4	−0.1	1.9
$BH_2Cl + Cl \rightarrow BHCl + HCl$	12.0	1.3	11.9	−0.7	−0.1	−2.0
$BHCl_2 + Cl \rightarrow BCl_2 + HCl$	12.5	1.8	12.4	0.0	−0.1	−1.8
chlorine abstractions transition states						
$BCl + H \rightarrow B + HCl$	28.4	20.4	43.5	26.0	15.1	5.6
$BH_2Cl + H \rightarrow BH_2 + HCl$	36.3	23.2	37.2	20.7	0.9	−2.5
$BHCl_2 + H \rightarrow BHCl + HCl$	33.3	20.3	41.5	25.1	8.2	4.7
$BCl_3 + H \rightarrow BCl_2 + HCl$	29.8	17.2	43.4	26.7	13.6	9.5

[a] At 0 K, MP2 values without ZPE, G2 values include ZPE. [b] Compare with ref 5, 2.9 kcal/mol calculated by MRCI/pVTZ+sp. [c] Second-order saddle point.

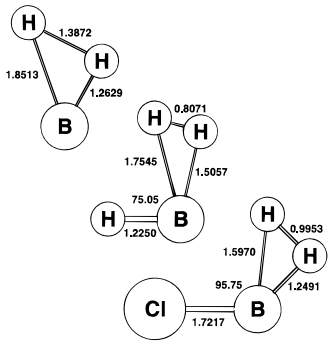

Figure 2. Transition states for the insertion of B, BH, and BCl into H_2 optimized at the MP2(full)/6-31G(d) level of theory.

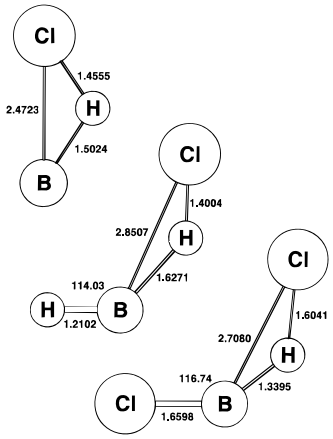

Figure 3. Transition states for the insertion of B, BH, and BCl into HCl optimized at the MP2(full)/6-31G(d) level of theory.

phase boron atom reported in some standard reference works (e.g., 133.3 kcal/mol in ref 25) is ca. 3 kcal/mol too low. The experimental value of 136.2 kcal/mol determined by Storms and Mueller[22] is supported by photoionization experiments[23] and by high-level calculations of Ochterski, Petersson, and Wiberg[24] and by our previous theoretical work.[3]

The transition states for insertion reactions of B, BH, and BCl into H_2 are shown in Figure 2. All of these insertion reactions have a strongly distorted, non-least motion transition structure because of orbital symmetry considerations similar to carbene and silylene insertions.[26] Like the carbene and silylene insertions,[26] these reactions show a profound increase in the barrier height on halogen substitution (4.6 kcal/mol for $BH + H_2$ versus 31.7 kcal/mol for $BCl + H_2$). The $BH + H_2 \rightarrow BH_3$ reaction has been studied previously at higher levels of theory. The MP2/6-31G(d) optimized transition state is ca. 0.1 Å earlier than the CASSCF/pVTZ-f structure;[5] the MRCI/pVTZ+sp barrier also occurs significantly earlier along the reaction path.[5] The barrier computed at the G2 level of theory is 1.7 kcal/mol higher than the MRCI/pVTZ+sp barrier. The latter is in excellent agreement with experiment.[5]

The transition states for the reaction of B, BH, and BCl with HCl shown in Figure 3 look more like abstractions, but the reaction path following confirms that these are insertion reactions. The reactants and transition states for B, BH, and BCl plus HCl lie 20−40 kcal/mol below the abstraction products, BH, BH_2, and BHCl plus Cl, because of the strength of the H-Cl bond being broken compared to the B−H bond being formed. By contrast, the insertion reactions are exothermic by 100−120 kcal/mol because two bonds are formed but only one is broken. Somewhat surprisingly, the approach of the reagents appears to be governed by the HCl hydrogen interacting with the boron lone pair rather than the chlorine lone pair interacting with the empty boron p orbital.

Figure 4 shows the hydrogen abstraction transition structures for $BH + H \rightarrow B + H_2$ and $BH_{3-n}Cl_n + H \rightarrow BH_{2-n}Cl_n + H_2$. No abstraction transition states could be found for $BH_{2-n}Cl_n + H$, since the lowest energy processes are barrierless H additions to form $BH_{3-n}Cl_n$. Each of the four structures of the stationary points shown in Figure 4 has a linear B−H−H moiety, with a planar boron and partially broken/formed B−H and H−H bonds. Because of the weakness of the BH bond, $BH + H \rightarrow B + H_2$ is quite exothermic (21.5 kcal/mol) and has a small barrier (4.3 kcal/mol). The other three abstraction reactions are thermoneutral and have barriers of ca. 12 kcal/mol. Even though the structures for $BH_2Cl + H \rightarrow BHCl + H_2$ and $BHCl_2 + H \rightarrow BCl_2 + H_2$ are first-order saddle points, the structure for BH_3

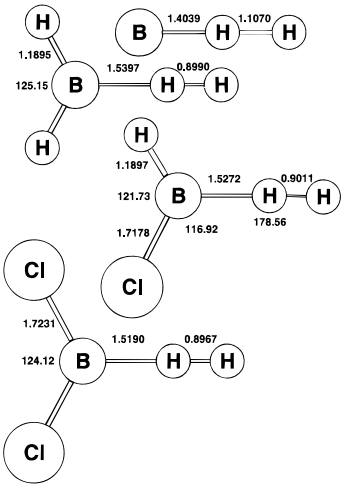

Figure 4. Hydrogen abstraction by H from BH, BH_3, BHCl, and $BHCl_2$ optimized at the MP2(full)/6-31G(d) level of theory. Note that BH_2-H-H is a second-order saddle point, but all other structures are first-order saddle points (transition states).

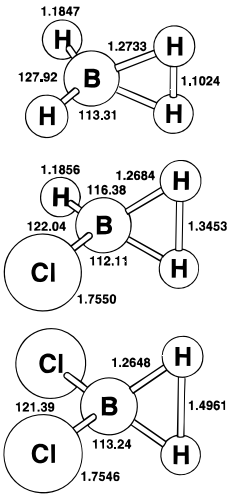

Figure 5. Intermediates for hydrogen addition to BH, BH_3, BHCl, and $BHCl_2$ optimized at the MP2(full)/6-31G(d) level of theory.

$+ H \rightarrow BH_2 + H_2$ is a second-order saddle point (two imaginary frequencies).

Further optimization reveals that the $BH_{3-n}Cl_n + H \rightarrow BH_{2-n}Cl_n + H_2$ reactions can proceed by a lower energy pathway involving H addition to form a $BH_{4-n}Cl_n$ intermediate followed by elimination of H_2.

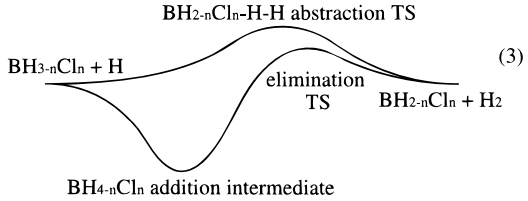

(3)

The hydrogen atom approaches along the axis of the empty p orbital on boron with little or no barrier to form a highly distorted tetracoordinate intermediate, as shown in Figure 5. The BH_4 structure is isoelectronic with CH_4^+ and SiH_4^+; each of these species suffers Jahn−Teller distortions[27] because each can be obtained by removing an electron from a triply degenerate orbital in tetrahedral BH_4^-, CH_4, or SiH_4. For BH_4, the lowest energy structure contains a three-membered ring with elongated B−H and H−H bonds and is ca. 15 kcal/mol more stable than $BH_3 + H$ or $BH_2 + H_2$. The structures of $BHCl-H_2$ and BCl_2-H_2 are analogous but are only ca. 7 and 4 kcal/mol more stable than the separated species.

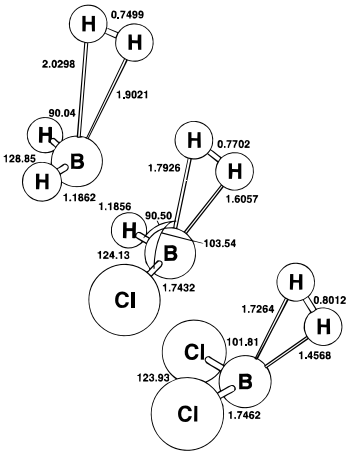

Figure 6. Transition states for the insertion of BH_2, BHCl, and BCl_2 into H_2 and the elimination of H_2 from the intermediates BH_2-H_2, $BHCl-H_2$, and BCl_2-H_2 optimized at the MP2(full)/6-31G(d) level of theory.

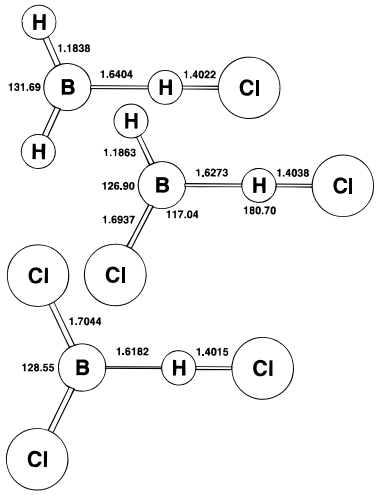

Figure 7. Transition states for hydrogen abstraction by Cl from BH, BH_3, BH_2Cl, and $BHCl_2$ optimized at the MP2(full)/6-31G(d) level of theory.

The elimination reaction $BH_{4-n}Cl_n \rightarrow BH_{2-n}Cl_n + H_2$ proceed via the transition states shown in Figure 6. The reverse of these reactions are insertions and behave similar to carbene and silylene insertion reactions,[26] $AXY + H_2 \rightarrow AH_2XY$, A = C, Si. The transition states are non-least motion and occur progressively later along the reaction path, and the insertion barriers increase with halogen substitution (0.4, 6.7, and 12.0 kcal/mol for BH_2, BHCl, and $BCl_2 + H_2$, respectively). For $BH_3 + H \rightarrow BH_2 + H_2$, the barrier for addition−elimination (1.1 kcal/mol) is considerably lower than direct abstraction (12.5 kcal/mol, second-order saddle point). However, for $BHCl_2 + H \rightarrow BCl_2 + H_2$, the two processes have nearly equal barriers and will be competitive (12.2 kcal/mol for addition−elimination vs 11.7 kcal/mol for abstraction).

For the divalent boron species, the $BH_{2-n}Cl_n + H \rightarrow BH_{1-n}Cl_n + H_2$ process also occurs by addition−elimination. Even though the reverse of the elimination step can have a large barrier (Figure 2, 4.6 kcal/mol for $BH + H_2$, but 31.7 kcal/mol for $BCl + H_2$), the overall process is quit exothermic (27.1 kcal/mol for $BH_2 + H \rightarrow BH + H_2$ and 45.4 kcal/mol for $BHCl + H \rightarrow BCl + H_2$) and there is no net barrier.

The transition states for the abstraction of H by Cl are shown in Figure 7. For $BH + Cl \rightarrow B + HCl$, the reaction is exothermic by 19.9 kcal/mol and appears to occur by a linear

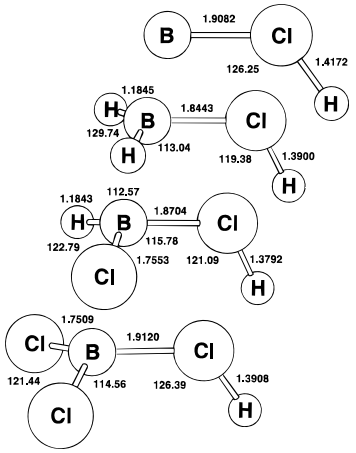

Figure 8. Transition states for chlorine abstraction by H from BCl, BH_2Cl, $BHCl_2$, and BCl_3 optimized at the MP2(full)/6-31G(d) level of theory.

approach without a barrier. The BH_2 and BHCl plus Cl reactions are exothermic (25.2 and 43.8 kcal/mol, respectively) and proceed by barrierless addition to form $BH_{2-n}Cl_{n+1}$ which can eliminate HCl (see Figure 3), with no net barrier. The $BH_{3-n}Cl_n + Cl \rightarrow BH_{2-n}Cl_n + HCl$ reactions are nearly thermoneutral with little or no barrier. An addition−elimination mechanism is also conceivable but would involve more extensive rearrangement than the $BH_{3-n}Cl_n + H \rightarrow BH_{2-n}Cl_n + H_2$ case.

The transition states for $BCl + H \rightarrow B + HCl$ and $BH_{3-n}Cl_n + H \rightarrow BH_{2-n}Cl_n + HCl$ are shown in Figure 8. In contrast to the abstraction reactions discussed above, these transition states have a bent B−Cl−H moiety. The reactions are endothermic by ca. 20 kcal/mol; the reverse barriers are relatively small but increase with increasing chlorine substitution. Reaction path following confirms that these are abstraction reactions.

Summary

Although the reactions in Figure 1 are numerous, they appear to involve only three simple classes: bond cleavage, radical abstraction, and insertion reactions. Closer examination, however, reveals a richer structure. Insertion reactions occur by highly distorted, non-least motion transition states. Insertion barriers increase with chlorine substitution on boron, whereas abstraction barriers are relatively insensitive. The transition states for the abstraction of hydrogen are linear, but those for the abstraction of chlorine are bent. Hydrogen abstraction by chlorine proceeds with little or no barrier, but hydrogen abstraction by hydrogen has a barrier of ca. 12 kcal/mol. The lowest energy pathway for the latter, $BH_{3-n}Cl_n + H \rightarrow BH_{2-n}Cl_n + H_2$, is not an abstraction but an addition−elimination mechanism via a tetracoordinate intermediate. Likewise, the divalent species undergo addition−elimination reactions, rather than abstractions. All of the transition structures have been characterized at the MP2(full)/6-31G(d) level and the barriers have been computed at the G2 level of theory. These calculations should provide a foundation for a detailed analysis of reaction rates in the BH_mCl_n system.

Acknowledgment. This work was supported by grants from the Office of Naval Research (for S.J.H., N00014-95-C-0155) and from the National Science Foundation (for H.B.S., CHE9400678).

References and Notes

(1) Olsson, M.; Stridh, B.; Jansson, U.; Carlsson, J.; Soderberg, S. *Mater. Sci. Eng.* **1988**, *A105*, 453. Gafri, O.; Grill, A.; Itzhak, D.; Inspektor, A.; Avni, R. *Thin Solid Films* **1980**, *72*, 523. Friesen, T.; Haupt, J.; Gissler, W.; Barna, A.; Barna, P. B. *Surf. Coatings Technol.* **1991**, *48*, 169.

(2) Rebenne, H.; Pollard, R. *J. Am. Ceramic Soc.* **1987**, *70*, 907.

(3) Schlegel, H. B.; Harris, S. J. *J. Phys. Chem.* **1994**, *98*, 11178.

(4) Rice, J. K.; Caldwell, N. J.; Nelson, H. H. *J. Phys. Chem.* **1989**, *93*, 3600.

(5) Caldwell, N. J.; Rice, J. K.; Nelson, H. H.; Adams, G. F.; Page, M. *J. Chem. Phys.* **1990**, *93*, 479.

(6) Jourdain, J. L.; Laverdet, G.; Le Bras, G.; Combourieu, J. *J. Chim. Phys.* **1981**, *78*, 253.

(7) Garrett, B. C.; Truhlar, D. G. *J. Am. Chem. Soc.* **1979**, *101*, 5207.

(8) Mayer, S. W.; Schieler, L.; Johnston, H. S. *11th Symposium (International) on Combustion*, [*Proceedings*]; The Combustion Institute: Pittsburgh, PA, 1967; p 837.

(9) Curtiss, L. A.; Jones, C.; Trucks, G. W.; Raghavachari, K.; Pople, J. A. *J. Chem. Phys.* **1990**, *93*, 2537.

(10) Curtiss, L. A.; Raghavachari, K.; Trucks, G. W.; Pople, J. A. *J. Chem. Phys.* **1991**, *94*, 7221.

(11) Curtiss, L. A.; Carpenter, J. E.; Raghavachari, K.; Pople, J. A. *J. Chem. Phys.* **1992**, *96*, 9030.

(12) Frisch, M. J.; Trucks, G. W.; Schlegel, H. B.; Gill, P. M. W.; Johnson, B. G.; Robb, M. A.; Cheeseman, J. R.; Keith, T.; Petersson, G. A.; Montgomery, J. A.; Raghavachari, K.; Al-Laham, M. A.; Zakrzewski, V. G.; Ortiz, J. V.; Foresman, J. B.; Cioslowski, J.; Stefanov, B. B.; Nanayakkara, A.; Challacombe, M.; Peng, C. Y.; Ayala, P. Y.; Chen, W.; Wong, M. W.; Andres, J. L.; Replogle, E. S.; Gomperts, R.; Martin, R. L.; Fox, D. J.; Binkley, J. S.; Defrees, D. J.; Baker, J.; Stewart, J. P.; Head-Gordon, M.; Gonzalez, C.; Pople, J. A. *GAUSSIAN 94*; Gaussian, Inc.: Pittsburgh PA, 1995.

(13) Hariharan, P. C.; Pople, J. A. *Theor. Chim. Acta* **1973**, *28*, 213 and references therein. Francl, M. M.; Pietro, W. J.; Hehre, W. J.; Binkley, J. S.; Gordon, M. S.; DeFrees, D. J.; Pople, J. A. *J. Chem. Phys.* **1982**, *77*, 3654. Frisch, M. J.; Pople, J. A.; Binkley, J. S. *J. Chem. Phys.* **1984**, *80*, 3265 and references therein. The 6-31G(d) and 6-31G(d,p) basis sets are the same as 6-31G* and 6-31G**, respectively.

(14) Schlegel, H. B. *J. Comput. Chem.* **1982**, *3*, 214. Peng, C.; Ayala, P. Y.; Schlegel, H. B.; Frisch, M. J. *J. Comput. Chem.* **1996**, *17*, 49.

(15) Pople, J. A.; Krishnan, R.; Schlegel, H. B.; Binkley, J. S. *Int. J. Quantum Chem., Quantum Chem. Symp.* **1979**, *13*, 225.

(16) Trucks, G. W.; Frisch, M. J.; Andres, J. L.; Schlegel, H. B. *J. Chem. Phys.*, submitted for publication.

(17) Gonzalez, C.; Schlegel, H. B. *J. Chem. Phys.* **1989**, *90*, 2154. Gonzalez, C.; Schlegel, H. B. *J. Phys. Chem.* **1990**, *94*, 5523.

(18) Møller, C.; Plesset, M. S. *Phys. Rev.* **1934**, *46*, 618. For a review: Bartlett, R. J. *Annu. Rev. Phys. Chem.* **1981**, *32*, 359.

(19) Pople, J. A.; Head-Gordon, M.; Raghavachari, K. *J. Chem. Phys.* **1987**, *87*, 5968.

(20) Pople, J. A.; Scott, A. P.; Wong, M. W.; Radom, L. *Isr. J. Chem.* **1993**, *33*, 345.

(21) Pople, J. A.; Schlegel, H. B.; Krishnan, R.; DeFrees, D. J.; Binkley, J. S.; Frisch, M. J.; Whiteside, R. A.; Hout, R. F.; Hehre, W. J. *Int. J. Quantum. Chem., Quantum Chem. Symp.* **1981**, *15*, 269.

(22) Storms, E.; Mueller, B. *J. Phys. Chem.* **1977**, *81*, 318.

(23) Ruscic, B.; Mayhew, C. A.; Berkowitz, J. *J. Chem. Phys.* **1988**, *88*, 5580.

(24) Ochterski, J. W.; Petersson, G. A.; Wiberg, K. B. *J. Am. Chem. Soc.* **1995**, *117*, 11299.

(25) Chase, M. W.; Davies, C. A.; Downey, J. R.; Frurip, D. J.; McDonald, R. A.; Szverud, A. N. *JANAF Thermochemical Tables* 3rd ed.; *J. Phys. Chem. Ref. Data* **1985**, *14*.

(26) Sosa, C.; Schlegel, H. B. *J. Am. Chem. Soc.* **1984**, *106*, 5847. Ignacio, E. W.; Schlegel, H. B. *J. Phys. Chem.* **1992**, *96*, 1620. Su, M.-D.; Schlegel, H. B. *J. Phys. Chem.* **1993**, *97*, 9981.

(27) For leading references see: Frey, R. F.; Davidson, E. R. *J. Chem. Phys.* **1988**, *88*, 1775; **1988**, *89*, 4227.

JP960347H